List of pdfcomments

Notes on the Diffusion Equation

Wednesday 22nd January, 2014

1 Introduction

Consider an arbitrary solution $u : \mathbb{X}\times\mathbb{T} \mapsto \mathbb{R}$ to the simple diffusion equation

$$\frac{\partial u}{\partial t} = \frac{\partial^2 u}{\partial x^2}\,. \tag{1}$$

A computationally feasible approach would be to first establish a sequence of discrete grid-points, $\vec{X} = [X_j]_{j\in\mathbb{J}}$, and thence summarise the continuum dynamics u by the coarse dynamics $\vec{U} = [U_j]_{j\in\mathbb{J}}$, where $U_j(t) := u(X_j, t)$ for all $t \in \mathbb{T}$. We may suppose that $\vec{U}$ evolves temporally according to some self-contained system

$$\dot{\vec{U}}(t) = \vec{g}(\vec{U}(t))\,. \tag{2}$$

Consequently, a link from the coarse dynamics $\vec{U}$ back to the continuum dynamics u might be provided by choosing an appropriate spatial mapping of the form

$$u := u(x, \vec{U}(t)). \tag{3}$$

Under this scheme, the linear diffusion equation (1) becomes

$$\frac{\partial u}{\partial \vec{U}} \cdot \vec{g} = \frac{\partial^2 u}{\partial x^2}\,. \tag{4}$$

Observe that the evolution of u now has nonlinear interactions with $\vec{U}$.

2 Centre Manifold Approximation

The original diffusion equation (1) admits eigensolutions of the form

$$\tilde{u}(x,t) = e^{\lambda t + ikx}\,, \tag{5}$$

which are physically realisable for real eigenvalues $\lambda = -k^2 \leq 0$ for corresponding eigenmode wavenumbers $\pm k$. As a consequence, the transient solutions corresponding to $\lambda < 0$ decay rapidly to the centre manifold corresponding to $\lambda = 0$.

This centre manifold can be found in practice by iteratively refining approximations to u. In particular, consider a series expansion of the form

$$u \;\sim\; \hat{u}_0 + \gamma\hat{u}_1 + \gamma^2\hat{u}_2 + \cdots\,, \tag{6}$$

for some parameter $0 \leq \gamma \leq 1$. Now, the constant eigensolution for $\lambda = 0$ implies a slow evolution for the coarse dynamics given by equation (2), which therefore admits a series expansion of the form

$$\dot{\vec{U}} \;\sim\; \gamma\vec{g}_1 + \gamma^2\vec{g}_2 + \cdots\,. \tag{7}$$

Hence, equation (4) may be decomposed at each order ℓ of the parameter γ, giving

$$\frac{\partial^2\hat{u}_0}{\partial x^2} \;=\; 0\,, \tag{8}$$

$$\frac{\partial^2\hat{u}_\ell}{\partial x^2} \;=\; \sum_{m=0}^{\ell-1}\frac{\partial\hat{u}_m}{\partial\vec{U}}\cdot\vec{g}_{\ell-m}\,, \quad \text{for } \ell = 1,2,\ldots\,. \tag{9}$$

3 Leading Approximation

The leading equation (8) admits any spatially piecewise linear function as a solution. Hence, in keeping with the discretisation imposed by the coarse dynamics of Section 1, let the spatial domain be partitioned into contiguous intervals, namely $\mathbb{X} = \bigcup_{j\in\mathbb{J}^+}\mathbb{I}_j$, where $\mathbb{I}_j := [X_{j-1}, X_j]$ and $\mathbb{J}^+ := \mathbb{J}\backslash\{\underline{J}\}$ with $\underline{J} := \inf\mathbb{J}$. Then, consider the piecewise linear approximation

$$\hat{u}_0 = \sum_{j\in\mathbb{J}^+}\chi_j(\xi_j U_j + (1-\xi_j)U_{j-1})\,, \tag{10}$$

with indicator $\chi_j(x) = 1$ (or 0) for $x \in \mathbb{I}_j$ (or $x \notin \mathbb{I}_j$), and linear interpolator $\xi_j(x) = \frac{x - X_{j-1}}{X_j - X_{j-1}}$. This particular approximation is chosen to be continuous across the internal interval boundaries, namely $X_j = \mathbb{I}_j \bigcap \mathbb{I}_{j+1}$ for $j \in \mathbb{J}^0 := \mathbb{J}^+ \backslash \{\bar{J}\}$, where $\bar{J} := \sup \mathbb{J}$. In general, it suffices to impose a continuity condition at the right-hand end of each interval, namely:

$$[u]_j = 0 \qquad \forall j \in \mathbb{J}^0 \,, \tag{11}$$

where $[u]_j := \lim_{\epsilon \to 0^+} u(X_j + \epsilon, t) - u(X_j - \epsilon, t)$. Unfortunately, this linear approximation is not smooth at the interval boundaries. For convenience, consider regular grid spacings of size $X_j - X_{j-1} = H$. Then, denoting $\partial u / \partial x$ as u', observe that

$$[\hat{u}_0']_j = \frac{1}{H}(U_{j+1} + U_{j-1} - 2U_j) \;=\; \frac{1}{H}\, \delta^2 \hat{u}_0 \big|_{X_j} \,, \tag{12}$$

for the centred difference $\delta u(x,t) := u(x + \frac{H}{2}, t) - u(x - \frac{H}{2}, t)$. However, this non-smoothness may be corrected at higher order by imposing a further internal boundary condition, namely

$$[u']_j = \frac{1 - \gamma}{H}\, \delta^2 u \big|_{X_j} \qquad \forall j \in \mathbb{J}^0 \,. \tag{13}$$

Consequently, smooth approximations are found in the limit as $\gamma \to 1$.

4 Linear Eigenmode Analysis

Consider a single eigenmode of the form (5) for some fixed, non-dimensionalised wavenumber $\kappa = kH > 0$. Thus, allowing for the partitioning of $\mathbb{X}$, let

$$\tilde{u} \;\sim\; \sum_{j \in \mathbb{J}^+} \chi_j a_j e^{i\kappa \xi_j} + \text{c.c.} \,, \tag{14}$$

for arbitrary, time–varying, complex coefficients $a_j = A_j + iB_j$. We now seek the 'spatial' evolution from interval to interval for the given wavenumber. The continuity condition (11) implies that

$$a_{j+1} - a_j e^{i\kappa \xi_j} + \text{c.c.} = 0 \,. \tag{15}$$

Similarly, the smoothness condition (13) implies that

$$ika_{j+1} - ika_j e^{i\kappa} + \text{c.c.} = \frac{1 - \gamma}{H} \left(a_{j+1} e^{i\kappa} + a_j - 2a_j e^{i\kappa} \right) + \text{c.c.} \,, \tag{16}$$

where continuity has also been invoked at the left-hand of the jth interval. In coefficient form, the update from the jth to $(j+1)$th segment is

$$\begin{bmatrix} 1 & 0 \\ fc & 1-fs \end{bmatrix} \begin{bmatrix} A_{j+1} \\ B_{j+1} \end{bmatrix} = \begin{bmatrix} c & -s \\ s+f(2c-1) & c-2fs \end{bmatrix} \begin{bmatrix} A_j \\ B_j \end{bmatrix}, \qquad (17)$$

where $c+is := e^{i\kappa}$ and $f := \frac{1-\gamma}{\kappa}$. Now, letting $a_{j+1} = \mu a_j$, the characteristic equation for the growth factor μ is

$$(1-fs)\left[\mu^2 - 2\frac{c-fs}{1-fs}\mu + 1\right] = 0\,, \qquad (18)$$

with roots given by

$$\mu \;=\; \beta \pm \sqrt{\beta^2-1} \quad \text{for } \beta \;=\; \frac{c-fs}{1-fs}\,. \qquad (19)$$

Observe that $\beta \leq 1$ since $c = \cos\kappa \leq 1$ and $1-fs = 1-(1-\gamma)\frac{\sin\kappa}{\kappa} \geq 0$. Thus, for $|\beta| < 1$, the factors are complex with magnitude $|\mu| = 1$, indicating marginally stable evolution of a_j. This includes the limiting case of $\gamma = 1$ ($f = 0$), for which $\mu = c \pm is = e^{\pm i\kappa}$. Likewise, $\mu = \pm 1$ for $\beta = \pm 1$, corresponding to $\kappa = n\pi$, $n = 0, 1, 2, \ldots$. Finally, for small regions near each $\kappa = (2n+1)\pi$, it is found that $\beta < -1$, resulting in two real factors, $\mu < -1$ and $-1 < \mu < 0$, indicating unstable (saddle) evolution. More precisely, these unstable regions occur when

$$\frac{\kappa}{2} < (1-\gamma)\tan\frac{\kappa}{2}\,, \qquad \kappa \neq n\pi\,. \qquad (20)$$

Thus, at equilibrium ($\gamma = 0$) there is an initial forbidden gap $\kappa \in (0, \pi)$ adjacent to the centre manifold wavenumber $\kappa = 0$ (see Figure 1), indicating that transient solutions decay to the centre manifold at a rate of at least $\lambda = -k^2 = -\frac{\pi^2}{H^2}$. It is this gap that provides robustness to nonlinear perturbations of the system about the equilibrium.

5 Linear Dual Space

Assume for convenience that there are $|\mathbb{J}| \geq 3$ discrete grid-points, and thus $|\mathbb{J}^+| \geq 2$ intervals. Then an appropriate inner product for spatially square-integrable fields u and v is given by

$$\langle u, v\rangle = \int_{X_{\underline{J}}}^{X_{\bar{J}}} uv\; dx = \sum_{j\in\mathbb{J}^+} \int_{\mathbb{I}_j} uv\; dx\,. \qquad (21)$$

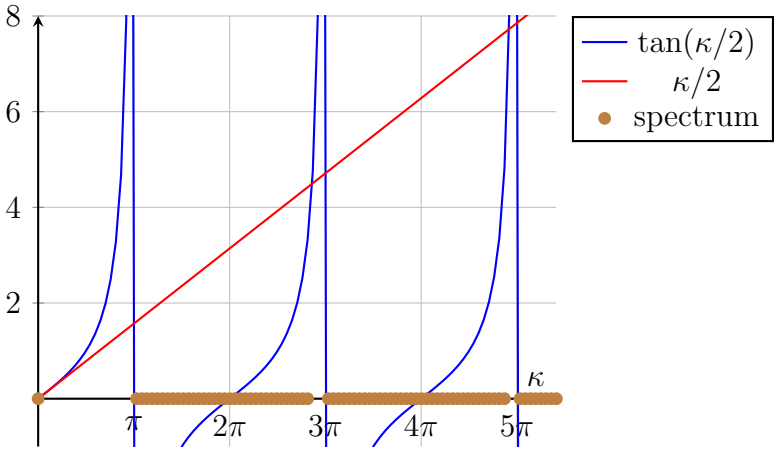

Figure 1: The equilibrium spectrum determined by the forbidding condition (20).

It can then be shown, for twice-differentiable fields, that

$$\langle u'', v\rangle = \langle u, v''\rangle + R\,, \tag{22}$$

with residual

$$R \;=\; \sum_{j\in\mathbb{J}^+} [r]_{X_{j-1}}^{X_j} = r_{\bar{J}} - r_{\underline{J}} - \sum_{j\in\mathbb{J}^0} [r]_j\,, \tag{23}$$

for $r = u'v - v'u$. Now, assuming that both u and v obey conditions (11) and (13), the residual jump at X_j becomes

$$\begin{aligned} [r]_j &= [u']_j V_j - [v']_j U_j \\ &= \frac{1-\gamma}{H}\left[(U_{j+1}+U_{j-1})V_j - (V_{j+1}+V_{j-1})U_j\right]\,. \end{aligned} \tag{24}$$

Observe that terms from surrounding intervals $\mathbb{I}_{j-1}$ and $\mathbb{I}_{j+1}$ will cancel terms from $\mathbb{I}_j$, leaving only contributions from the outermost boundary intervals $\mathbb{I}_{\underline{J}+1}$ and $\mathbb{I}_{\bar{J}}$; consequently:

$$\begin{aligned} R \;=\;& u'_{\bar{J}}V_{\bar{J}} - v'_{\bar{J}}U_{\bar{J}} - u'_{\underline{J}}V_{\underline{J}} + v'_{\underline{J}}U_{\underline{J}} \\ & - \frac{1-\gamma}{H}\left[U_{\bar{J}}V_{\bar{J}-1} - V_{\bar{J}}U_{\bar{J}-1} + U_{\underline{J}}V_{\underline{J}+1} - V_{\underline{J}}U_{\underline{J}+1}\right]\,. \end{aligned} \tag{25}$$

On a finite domain, there are three main outer boundary conditions that lead to a zero residual:

periodic Having period $\bar{J} - \underline{J}$ corresponds to $U_{\bar{J}} = U_{\underline{J}}$. Furthermore, by joining the domain cylindrically at $X_{\underline{J}}$ and $X_{\bar{J}}$, it can be shown that

$$u'_{\underline{J}} - u'_{\bar{J}} = [u']_{\bar{J}} = \frac{1-\gamma}{H}(U_{\underline{J}+1} + U_{\bar{J}-1} - 2U_{\bar{J}})\,, \tag{26}$$

using condition (13). Hence, $R = 0$ if correspondingly v is periodic with period $\bar{J} - \underline{J}$.

Dirichlet Setting $u = 0$ at the boundaries corresponds to $U_{\underline{J}} = U_{\bar{J}} = 0$, giving $R = 0$ if correspondingly $v = 0$ on the boundaries.

Neumann Requiring $u' = 0$ on the boundaries (for $\gamma = 1$) corresponds to

$$u'_{\underline{J}} = \frac{1-\gamma}{H}(U_{\underline{J}+1} - U_{\underline{J}})\,, \qquad u'_{\bar{J}} = \frac{1-\gamma}{H}(U_{\bar{J}} - U_{\bar{J}-1})\,, \tag{27}$$

giving $R = 0$ if correspondingly $v' = 0$ on the boundaries.

Under any of the above three conditions, observe that $\langle \mathcal{L}u, v\rangle = \langle u, \mathcal{L}v\rangle$ for $\mathcal{L} = \partial^2/\partial x^2$, and hence $\mathcal{L}$ is self-adjoint. Furthermore, we are free to choose any dual v, e.g. to satisfy $\mathcal{L}v = 0$ for conenience. In particular, we may specifically target the j-th interval for u by selecting $v = \hat{v}_0^{[j]}$, where

$$\hat{v}_0^{[j]} := \chi_j \xi_j + \chi_{j+1}(1 - \xi_{j+1}) \quad \forall j \in \mathbb{J}^0\,. \tag{28}$$

Observe that this dual satisfies conditions (11) and (13) for $\gamma = 0$. It can then be shown in general that

$$\langle u'', \hat{v}_0^{[j]}\rangle = -[u']_j + \frac{1}{H}\,\delta^2 u\big|_{X_j}\,, \tag{29}$$

for any continuous, twice-differentiable field u.

6 First-order Approximation

Substituting the leading approximation (10) into the nonlinear diffusion equation (9) for $\ell = 1$ results in the first-order equation

$$\hat{u}''_1 = \sum_{j\in\mathbb{J}^+} \chi_j(\xi_j g_{1,j} + (1-\xi_j) g_{1,j-1})\,. \tag{30}$$

Spatial integration then gives

$$\hat{u}_1' = \frac{H}{2}\sum_{j\in\mathbb{J}^+}\chi_j(\xi_j^2 g_{1,j} - (1-\xi_j)^2 g_{1,j-1} + c_{1,j})\,, \tag{31}$$

$$\hat{u}_1 = \frac{H^2}{6}\sum_{j\in\mathbb{J}^+}\chi_j(\xi_j^3 g_{1,j} + (1-\xi_j)^3 g_{1,j-1} + 3\xi_j c_{1,j} + d_{1,j})\,. \tag{32}$$

Recall from the chosen spatial discretisation that $u|_{X_j} = U_j$ at each grid-point. Observe this is already satified by $\hat{u}_0$ from equation (10), implying from expansion (6) that

$$\hat{u}_\ell|_{X_j} \equiv 0 \qquad \text{for } \ell = 1, 2, \ldots\,. \tag{33}$$

Thus $[\hat{u}_\ell]_j = 0$, satisfying the continuity condition (11), and furthermore $\delta^2\hat{u}_\ell|_{X_j} = 0$. Now, evaluating equation (32) at $\xi_j = 0$ gives $d_{1,j} = -g_{1,j-1}$, and at $\xi_j = 1$ gives $3c_{1,j} = -(g_{1,j} - g_{1,j-1})$. Thus, from equation (31), observe that

$$[\hat{u}_1']_j = -H\left(1 + \frac{1}{6}\delta^2\right) g_{1,j}\,. \tag{34}$$

However, the smoothness condition (13) gives

$$[\hat{u}_1']_j = \frac{1}{H}\,\delta^2\hat{u}_1\big|_{X_j} - \frac{1}{H}\,\delta^2\hat{u}_0\big|_{X_j} = -\frac{1}{H}\delta^2 U_j\,, \tag{35}$$

and hence

$$\left(1 + \frac{1}{6}\delta^2\right) g_{1,j} = \frac{1}{H^2}\delta^2 U_j\,. \tag{36}$$

This solution can also be otained more directly via the dual space by computing $\langle \hat{u}_1'', \hat{v}_0^{[j]}\rangle$ from equations (28) and (30), and using results (29) and (35).

Consequently, as a first approximation, the coarse dynamics evolve according to

$$\dot{\vec{U}} = \frac{\gamma}{H^2} S\delta^2\vec{U} + \mathcal{O}(\gamma^2)\,, \tag{37}$$

from equations (2) and (7), where, for convenience, we let $S := (1 + \frac{1}{6}\delta^2)^{-1}$. Now, recall from Section 2 that the eigensolution $\tilde{u}(x,t) = e^{\lambda t + ikx}$ to the diffusion equation (1) has the exact spectrum $\lambda = -k^2$. It can further be

shown that this eigensolution satisfies the relation $\delta^2\tilde{u} = -2(1-c)\tilde{u}$, where, as before, $c := \cos kH$. Hence, the spectrum of the first-order approximation with $\gamma = 1$ is given by

$$\lambda = -\frac{6(1-c)}{H^2(2+c)} \sim -k^2 - \frac{1}{12}H^2k^4 + \mathcal{O}(H^4k^6)\,, \tag{38}$$

which reveals an error of size $\mathcal{O}(H^2k^4)$ in comparison to the exact spectrum.

The behaviour of this approximate spectrum is shown in Figure 2. Observe that the second turning point of the approximation occurs at $k = \frac{\pi}{H}$, corresponding to $c = -1$. Hence, from the left-hand side of equation (38), we obtain $\lambda = -\frac{12}{H^2}$, in contrast to the true value of $\lambda = -\frac{\pi^2}{H^2}$, giving an error of $\Delta\lambda \approx -\frac{2.1}{H^2}$. Using the right-hand side of equation (38) instead leads to an approximate error estimate of $\Delta\lambda \approx -\frac{\pi^4}{12H^2} \approx -\frac{8.1}{H^2}$.

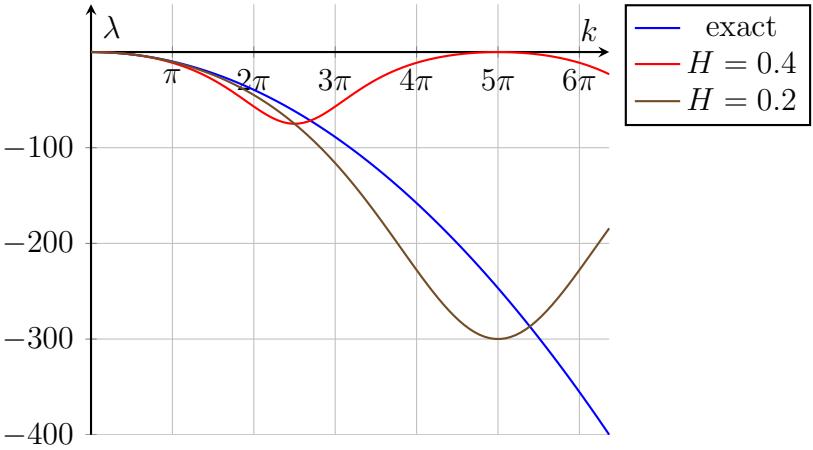

Figure 2: The exact spectrum (λ versus k) of the linear diffusion equation, compared to a first-order approximation with $H = 0.4$ and $H = 0.2$ for $\gamma = 1$.

Alternatively, suppose for the sake of argument that $X_j \equiv jH$. Then the continuum eigenmode $\tilde{u}(x,t) = e^{\lambda t + i\pi x/H}$ gives rise to a sawtooth mode in the coarse dynamics of the form $\tilde{U}_j = e^{\lambda t}(-1)^j$. It can then be shown that $\tilde{U}_j$ obeys the relation $\delta^2\tilde{U}_j = -4\tilde{U}_j$, and satisfies equation (37) for $\gamma = 1$ with a decay rate of $\lambda = -\frac{12}{H^2}$, the same as above.

7 Second-order Approximation

For convenience, consider the shift operator $\sigma u(x,t) := u(x+H,t)$; whence $\delta := \sigma^{1/2} - \sigma^{-1/2}$. Then, from equation (9) for $\ell = 2$, we obtain

$$\begin{aligned}\hat{u}_2'' &= \frac{\partial \hat{u}_0}{\partial \vec{U}} \cdot \vec{g}_2 + \frac{\partial \hat{u}_1}{\partial \vec{U}} \cdot \vec{g}_1 \\ &= \sum_{j\in\mathbb{J}^+} \chi_j \left\{\xi_j + (1-\xi_j)\sigma^{-1}\right\} g_{2,j} \\ &\quad - \frac{1}{6} \sum_{j\in\mathbb{J}^+} \chi_j \xi_j (1-\xi_j) \left\{(2-\xi_j)\sigma^{-1} + (1+\xi_j)\right\} S\delta^2 g_{1,j}\,, \end{aligned} \tag{39}$$

using equations (10) , (32), and (36). Next, observe from equations (29), (13) and (33) that

$$\langle \hat{u}_\ell'', \hat{v}_0^{[j]} \rangle \equiv 0 \qquad \text{for } \ell = 2, 3, \ldots\,. \tag{40}$$

Alternatively, it can be shown by direct integration and simplification that

$$\langle \hat{u}_2'', \hat{v}_0^{[j]} \rangle = HS^{-1} g_{2,j} - \frac{H}{6}\left(\frac{7}{60}\delta^2 + \frac{1}{2}\right) S\delta^2 g_{1,j}\,, \tag{41}$$

from equations (28) and (39). Hence, as a second approximation, the coarse dynamics evolve according to

$$\dot{\vec{U}} = \frac{\gamma}{H^2} S\delta^2 \vec{U} + \frac{\gamma^2}{60H^2}(7-2S)S^2\delta^4\vec{U} + \mathcal{O}(\gamma^3)\,, \tag{42}$$

using the fact that $S\delta^2 = 6(1-S)$.

Thus, following Section 6, the approximate spectrum for $\gamma = 1$ is now

$$\lambda = -\frac{1}{5H^2}\frac{96 + 27c - 72c^2 - 51c^3}{8 + 12c + 6c^2 + c^3} \sim -k^2 - \frac{1}{180}H^4k^6 + \mathcal{O}(H^6k^8)\,. \tag{43}$$

Observe that the $\mathcal{O}(H^2k^4)$ error term from the first-order approximation (38) has now been completely eliminated by the second-order correction, in favour of an $\mathcal{O}(H^4k^6)$ error. This adjusted spectral behaviour is shown in Figure 3. Observe that the turning point again occurs at $k = \frac{\pi}{H}$. Hence, as per Section 6, the sawtooth mode (with $c = -1$) now has a decay rate of $\lambda = -\frac{48}{5H^2}$, leading to an error of $\Delta\lambda \approx \frac{0.27}{H^2}$, which is an order of magnitude smaller than the first-order error.

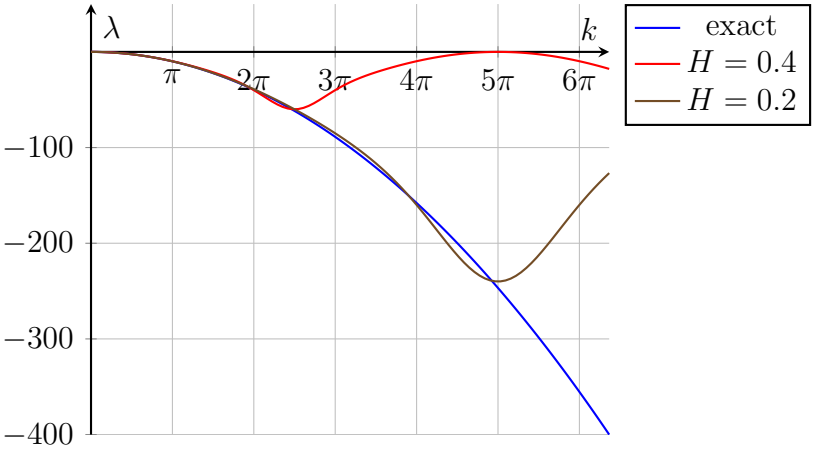

Figure 3: The exact spectrum (λ versus k) of the linear diffusion equation, compared to a second-order approximation with $H = 0.4$ and $H = 0.2$ for $\gamma = 1$.